Boron solution and distribution in α-Fe: Application to boron steel

Seung Su Baik and B. I. Min*
Department of Physics, PCTP, Pohang University of Science and Technology, Pohang 790-784, Korea

S. K. Kwon† and Y. M. Koo
Graduate Institute of Ferrous Technology, Pohang University of Science and Technology, Pohang 790-784, Korea

(Received 16 October 2009; revised manuscript received 23 February 2010; published 1 April 2010)

Formation-energy formalism for a general interface is developed and applied to α-Fe host with boron (B) impurities. In bulk α-Fe, B impurities prefer to be located at substitutional position rather than at interstitial. The estimated formation energy of substitutional B is lower than that of interstitial B by 0.10 eV in the dilute impurity limit. At the surface, however, the interstitial site is found to be preferred, and B impurities on top of the surface are the most stable as compared to those in the subsurface positions. The stability of B impurities increases as they get close to the free surface, indicating that B impurities tend to segregate toward the free surface. This surface segregation of B impurities is found to be the direct reflection of the surface-energy minimization of Fe-B system. Based on the first-principles band calculations, it is deduced that the dominant B diffusion behavior near the free surface is described by the interstitial-to-interstitial diffusion mechanism.

DOI: 10.1103/PhysRevB.81.144101 PACS number(s): 61.72.−y, 75.50.Bb, 89.20.Bb

I. INTRODUCTION

It is well known that the hardenability of steels can be greatly enhanced by the addition of trace boron (B) to steels.[1,2] This effect is related to the thermal diffusion and segregation of boron to the grain boundaries in the cooling process.[3–5] However, along with the positive and negative aspects of boron addition in ferritic steels,[6–8] a long debate over the occupation type of boron solution in α-Fe is unresolved yet and understanding of diffusion mechanism is still missing. There are three different proposals on the boron solution in α-Fe: (i) boron exists in a substitutional type,[9–12] (ii) boron exists in an interstitial type,[13–16] and (iii) boron solution can be both types[17] and stabilized with other impurity elements such as Ni, C, and N.[18,19] The experimental difficulties in figuring out the boron-solution-type arise mainly from the low solubility of boron and other impurity contribution such as O and C to the measurements. These two factors are inevitably related to the purity of examining Fe-B alloys.[19] In the geometrical analysis, the atomic dimension of B is in the midway between the host atom and other alloying elements such as C and N, and so it is possible to explore its effects as both interstitial and substitutional impurities during alloying formation. In fact, although B is just beside C in the periodic table, its behaviors in Fe host and the entailing physical properties are totally different from C. However, the reason of its distinct behaviors is not resolved yet.

In this paper, we have addressed the issues of boron solution, distribution, and diffusion behaviors in boron steel. For this purpose, we have theoretically investigated various boron solutions in α-Fe, checking the boron formation energies both in the bulk and at the (100) surface. For comparison, we have also studied the physical properties of C and N impurities in α-Fe. General formalism for the formation-energy calculation in slab geometry is developed and applied to the estimation of boron formation energy. In the formula, the slab formation energy is reinterpreted in relation with surface energy and bulk formation energy. We shifted the interpretation of surface stability from the viewpoint of formation energy to that of surface energy. The formalism is general and applicable to arbitrary interfaces such as a grain boundary. We show that boron inside the bulk prefers the substitutional position but the preferential position changes when the free surface is introduced. In bulk α-Fe, the effect of competition between geometry and chemical bonding on impurity solution type and its solubility is discussed. In slab α-Fe, the effect of geometrical pressure and its relaxation induced by the free surface on B impurity is discussed. Further, both bulk and surface magnetism of Fe-B alloy systems are investigated.

II. COMPUTATIONAL METHOD

To simulate the boron distribution in α-Fe, we employed the full-potential linearized augmented plane-wave band method[20] implemented in WIEN2K package.[21] The generalized gradient approximation[22] is used for the exchange-correlation potential. The muffin-tin (MT) radii of Fe, B, C, and N atoms are chosen as 1.8 a.u., 1.4 a.u., 1.2 a.u., and 1.2 a.u., respectively. Wave functions inside the muffin-tin spheres are expanded in spherical harmonics up to $l=10$, and Fe $3s$ and $3p$ semicore local orbitals are included in the basis set. The wave function in the interstitial region is expanded with plane waves up to $K\,\max=3.5$ and 3.2 a.u.$^{-1}$ for bulk and surface slab calculation, respectively. The charge densities are described with plane waves up to $G\,\max=16\sqrt{\mathrm{Ry}}$. The equilibrium lattice constant of $a=5.35$ a.u. (2.83 Å) from the primitive cell calculation was used for the supercell construction. For the bulk calculations, $2\sqrt{2}\times2\sqrt{2}\times3$ supercells with 48 Fe atoms were considered. For (100) surface calculations, 2×2 supercell with 15 layers were constructed. The thickness of inserted vacuum corresponds to four atomic layers. In all calculations, the atomic relaxations are terminated when the forces in all atomic sites are less than 2 mRy/a.u.

 ©2010 The American Physical Society

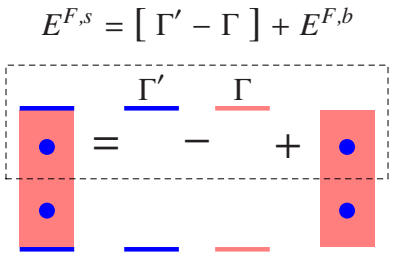

FIG. 1. (Color online). Decomposition of the formation energy of Fe_nX slab system into the surface contribution plus bulk formation energy. Filled rectangle and circle represent bulk Fe host and X impurity inside it. Each thick line represents the surface with or without impurity.

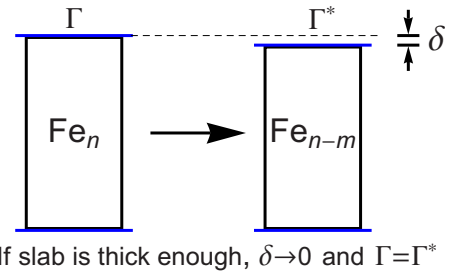

FIG. 2. (Color online). Surface-energy equality of two slab systems, Fe_n and Fe_{n-m}. With large n, the thickness difference of two slabs is negligible, and the surface energies of two systems are equal.

III. FORMALISM

From general consideration, the formation energy E^F of bulk (b) and slab $(s)Fe_nX_m$ system with n Fe and m X impurities can be written as

$$E^{F,b/s} = E^{b/s}(Fe_nX_m) - E^{b/s}(Fe_n) - mE(X), \tag{1}$$

where $E^{b/s}(Fe_nX_m)$, $E^{b/s}(Fe_n)$, and $E(X)$ are the total energies of corresponding systems in their ground states. Although computational procedure of E^F looks straightforward with this formula, it is not the case for slab system with substitutional impurities. For example, when we consider $Fe_{n-1}X$ slab system with one substitutional impurity, construction of the slab supercell for $E^s(Fe_{n-1})$ will fail to be accomplished because the surface sets the geometrical constraints for possible atomic arrangement. To overcome this obstacle, we decompose $E^s(Fe_nX_m)$ and $E^s(Fe_n)$ into their surface and bulk contributions,

$$E^s(Fe_nX_m) = \Gamma' + E^b(Fe_nX_m),$$

$$E^s(Fe_n) = \Gamma + E^b(Fe_n), \tag{2}$$

where Γ' and Γ are the surface energies of Fe_nX_m and Fe_n slabs, respectively. The surface area, A, of given supercell is absorbed in Γ' and Γ. It should be noted that the impurity effect on the surface energy is included in Γ' but not in Γ. The decomposition of Eq. (2) can be applied to both interstitial and substitutional impurities with arbitrary m and large n. Hence, by substituting Eq. (2) into Eq. (1), the slab formation energy can be analyzed into surface-energy difference plus bulk formation energy,

$$E^{F,s} = [\Gamma' - \Gamma] + E^{F,b}. \tag{3}$$

In Fig. 1, a schematic of this decomposition is provided for an intuitive understanding. Equation (3) can be extended with generality to an arbitrary interface geometry such as a grain boundary, for which the interface formation energy can be obtained from the sum of the interface energy difference and the bulk formation energy.

When m impurities are introduced at interstitial sites in Fe_n host system, the total number of host atoms remains n while that becomes $n-m$ when m X impurities are substitutional. More specifically for the substitutional impurities, $E^s(Fe_{n-m}) = \Gamma + E^b(Fe_{n-m})$ and $E^b(Fe_{n-m}) = (n-m)/n \times E^b(Fe_n)$. Since the surface energies of two slab systems, Fe_n and Fe_{n-m}, are equal with a large n as depicted in Fig. 2,

$$\Gamma = E^s(Fe_n) - E^b(Fe_n) = E^s(Fe_{n-m}) - E^b(Fe_{n-m}), \tag{4}$$

the ground-state energy of Fe_{n-m} slab system can be rewritten as

$$\begin{aligned} E^s(Fe_{n-m}) &= \Gamma + E^b(Fe_{n-m}) \\ &= \Gamma + (n-m)/n[E^s(Fe_n) - \Gamma] \\ &= (m/n)\Gamma + (n-m)/nE^s(Fe_n). \end{aligned} \tag{5}$$

Therefore, our final expression of formation energy for the m substitutional impurities in a slab system becomes

$$\begin{aligned} E^{F,s} = {} & E^s(Fe_{n-m}X_m) \\ & - [(m/n) \times \Gamma + (n-m)/n \times E^s(Fe_n)] - mE(X). \end{aligned} \tag{6}$$

In the dilute limit of a large n, the first term in the square bracket can be ignored. However, in usual slab calculations where the total number of atoms is comparable to 10^2 in order of magnitude, this extra term is non-negligible. For example, the total surface energy of 11-layered slab with 99 Fe atoms is about 14.4 eV (1.6 eV/surface atom). Then, the contribution of the extra term to the formation energy amounts to $14.4/(99/2) = 0.29$ eV per impurity, which is significant in size.

IV. RESULT AND DISCUSSION

A. Bulk result

We have calculated formation energies for various types of impurities in bulk α-Fe. Here, the formation energies are obtained by replacing the ground-state energy of impurity X, $E(X)$, in Eq. (1) by the atomic energy of corresponding impurity. This replacement gives rise to only a constant energy shift. When we use the true ground-state energy for each impurity, the formation energies become positive for all B, C, and N impurities, implying that the solubility is zero at $T=0$ K. For C, the positive formation energy is consistent with existing report.[23] To determine true solubility, one must consider configurational (mixing) and thermal (vibrational) entropy,[17,24] which lower the total free energy at the expense of internal energy increment. However, we can still derive

TABLE I. Formation energies (electron volt), $E_{\mathrm{I}}^{F,b}$ and $E_{\mathrm{S}}^{F,b}$, and formation-energy difference, $\Delta E=E_{\mathrm{S}}^{F,b}-E_{\mathrm{I}}^{F,b}$, between substitutional and interstitial sites for X=B,C,N impurities in Fe_{48} bulk host. S and I represent substitutional and interstitial, respectively.

X		B	C	N
$E_{\mathrm{I}}^{F,b}$		−5.20	−5.94	−2.65
$E_{\mathrm{S}}^{F,b}$		−5.37	−3.85	0.04
	Present	−0.17	2.09	2.69
ΔE	Ref. 17	−0.13	2.26	
	Ref. 26		2.37	2.89

physically meaningful result at low-temperature limit from the difference of formation energies between substitutional and interstitial sites, $\Delta E=E_{\mathrm{S}}^{F,b}-E_{\mathrm{I}}^{F,b}$. This allows us to determine relative stability between the two sites for impurity to reside in. Here we denote the substitutional and the interstitial (octahedral site) case by S and I, respectively. Tetrahedral site is excluded due to its less stability than octahedral site.[25]

Estimated formation energies and ΔE values are summarized in Table I. Note that ΔE is negative for B, distinctly from positive ΔE's for C and N, implying that the B impurities favor substitutional sites while C and N impurities favor interstitial sites. ΔE's for B, C, and N are −0.17 eV, 2.09 eV, and 2.69 eV, respectively. The different feature of B from C and N is understandable by considering that the atomic radius of B is much larger than those of C and N: r_X =0.94 Å, 0.77 Å, and 0.72 Å for X=B, C, and N, respectively. A larger atomic size of B impurity entails the larger displacements of the neighboring Fe atoms. Hence, as can be deduced, the substitutional occupancy of boron seems reasonable due to its relatively large size. The above-mentioned ΔE values are obtained from Fe_{48} supercell calculation. When we used a smaller (larger) Fe_{24} (Fe_{72}) host supercell, we obtained slightly different values of ΔE=−0.26 (−0.15) eV for B impurity, reflecting the finite supercell size effect. In overall, with increasing the supercell size, the absolute value of ΔE decreases with the same negative sign. An extrapolation with inverse proportional function[27] results in ΔE_0=−0.10 eV in the dilute limit of B impurity corresponding to the experimentally observed parts per million level concentration.[5,19,28] Therefore, at low concentration, the substitutional B is more stable than the interstitial B by 0.10 eV.

This finding, however, does not necessarily mean that, inside the bulk, the substitutional-to-substitutional diffusion mechanism is more effective than the interstitial-to-interstitial diffusion mechanism.[17] In fact, the substitutional diffusion can hardly occur if the neighboring site is not vacant, and hence the vacancy concentration plays a crucial role in determining the dominant diffusion mechanism. The vacancy concentration is a still sensitive and controversial issue. However, employing the estimated vacancy concentrations,[18,19] 10^{-7}–10^{-9}, it is thought that the substitutional diffusion cannot be ignored and both diffusion mechanisms should be considered inside the bulk.

Figure 3 shows the lattice volume effect on the formation energy of B impurity in α-Fe. Noteworthy is that, just above the equilibrium lattice constant 2.83 Å, ΔE becomes positive, indicating that the interstitial B becomes more stable than the substitutional B. This feature can be understood in terms of the enlarged interstitial space with lattice expansion at which B can be located. Consequently, it is implied that the interstitial-to-interstitial diffusion can be more probable than the substitutional-to-substitutional diffusion at elevated temperature.

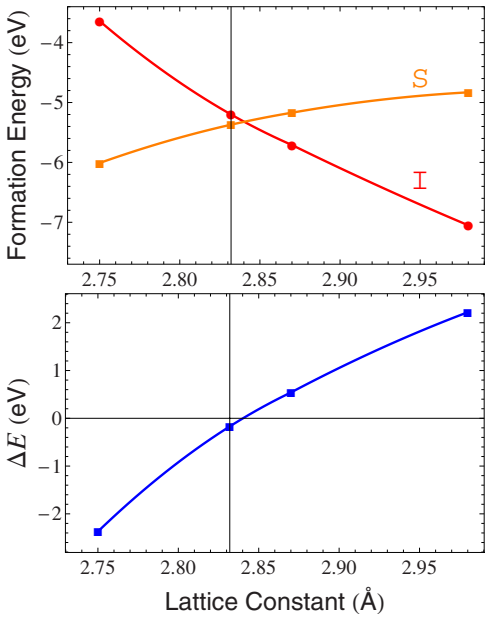

FIG. 3. (Color online). Formation energies, $E_{\mathrm{I}}^{F,b}$ and $E_{\mathrm{S}}^{F,b}$ vs lattice constant, and formation-energy difference, $\Delta E=E_{\mathrm{S}}^{F,b}-E_{\mathrm{I}}^{F,b}$ vs lattice constant for B impurity in α-Fe. I and S represent interstitial and substitutional, respectively. The equilibrium lattice constant is at the vertical line.

To understand detailed bonding characteristics, we provide the partial density of states (PDOS) for B, C, and N impurities in α-Fe at the equilibrium lattice constant in Fig. 4. The PDOSs manifest that the hybridizations between Fe 3d and X 2p (X=B,C,N) states are larger for the interstitial X than for the substitutional X. The blue dashed lines in Figs. 4(a)–4(c) show that the energy ranges of strong hybridizations between Fe 3d and X 2p (X=B,C,N) states decrease in B-C-N order. The hybridization bondings are prominent for the interstitial B, C, and N for the energy ranges of −7–−4 eV, −8–−5 eV and −9–−6 eV, respectively. By these hybridizations, small portions of Fe 3d states are shifted toward the lower-energy ranges, thereby lowering the total energies of Fe-X systems. In fact, the bonding strength is found to become larger in B-C-N order, as indicated by the decreasing X-Fe (X=B,C,N) distance from 3.39, 3.28 to 3.25 a.u.. Hence, for the interstitial case, the available energy gain for B-Fe bonding is much smaller than those for C-Fe and N-Fe bonding. This explains that the solubility of the interstitial impurity X increases in B-C-N order in α-Fe, that is, Fe does not like B so much as C and N. On the other hand, for the substitutional cases, these energy ranges of strong hybridizations do not appear as shown in Figs. 4(d)–4(f). The X-Fe (X=B,C,N) distance are found to be 4.52, 4.46 to 4.47 a.u., and so the hybridization bondings are much less than those for the interstitial cases.

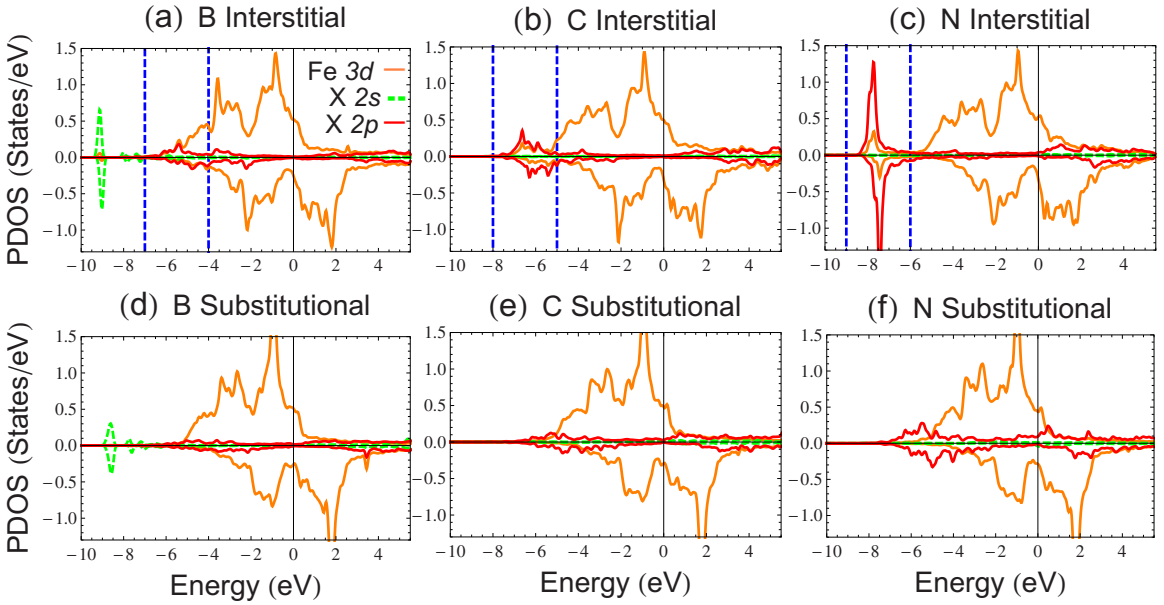

FIG. 4. (Color online). (a) PDOS for interstitial B in α-Fe. (b) PDOS for interstitial C in α-Fe. (c) PDOS for interstitial N in α-Fe. (d) PDOS for substitutional B in α-Fe. (e) PDOS for substitutional C in α-Fe. (f) PDOS for substitutional N in α-Fe. Blue dashed lines in (a), (b), and (c) show the energy ranges of strong hybridizations between Fe $3d$ and X $2p$ (X=B,C,N) states.

The bond charge density (valence charge density minus superposition of atomic charge densities) in Fig. 5 exhibits the similar bonding characters. The bond charge density arises from the charge transfer between compositional atoms when formed in solids, and so represents the effective bond density. It is clearly seen that the positive bond densities around the interstitial X are still more populated than those for the substitutional X, indicating that interstitial X-Fe bondings are much stronger than substitutional X-Fe bondings. As expected, the contour deformation of positive bond density around interstitial B is larger than those for interstitial C and N due to relatively big size of B impurity. As going from B to N, more positive bond densities are populated, implying that X-Fe bonding strength increases in B-C-N order. It is noteworthy that the positive bond density of substitutional B is localized at its core region whereas those of substitutional C and N are more or less delocalized in the interstitial region. This feature implies that the substitutional B in bulk Fe exhibits totally different behavior from C and N.

A bit larger bonding strengths and smaller sizes of C and N than B would induce the larger displacements of neighboring Fe atoms, resulting in more formation energy loss for substitutional C and N than for substitutional B impurity. That is why C and N impurities favor the interstitial sites while B favors the substitutional sites. These analyses suggest that the stability of impurity is effectively determined by the structural geometry of the host and the atomic dimension of impurity itself. The specific chemical configuration of the impurity is not a dominant factor. When impurities are dissolved into host system, the dual properties of geometry and chemical bonding always compete. The structure of host material and atomic dimension of impurity are geometrical factors, and the number of valence electrons and electronegativity are chemical bonding factors. The impurity solution type is prominently determined by geometrical factors and, once it is determined, the impurity solubility is cooperatively determined by geometrical and chemical factors. As studied above, B, C, and N impurities in Fe host comply with this rule.

B. Surface result

To examine the boron distribution at the surfaces of α-Fe, we have considered a boron impurity in the 15-layer Fe slab with (100) surface orientation. The formation energies and surface energies, which are obtained from the formulas de-

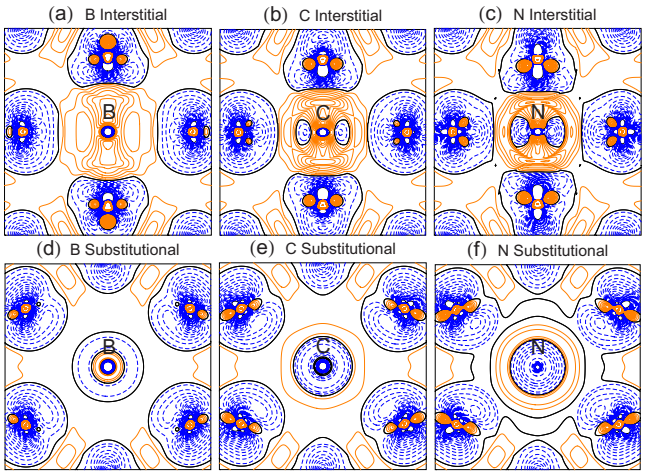

FIG. 5. (Color online). (a) Bond charge density (valence charge density—superposition of atomic charge densities) for interstitial B. (b) Bond charge density for interstitial C. (c) Bond charge density for interstitial N. (d) Bond charge density for substitutional B. (e) Bond charge density for substitutional C. (f) Bond charge density for substitutional N. Solid (orange) and dashed (blue) lines stand for positive and negative bond densities, respectively.

TABLE II. $E_{\mathrm{I}}^{F,s}$ and $E_{\mathrm{S}}^{F,s}$ are the formation energies (electron volt) and $\gamma_{\mathrm{I}}'(=\Gamma_{\mathrm{I}}'/A)$ and $\gamma_{\mathrm{S}}'(=\Gamma_{\mathrm{S}}'/A)$ are the surface energies per unit area (joule per meter square) for 15-layer Fe slabs with interstitial and substitutional B impurity, respectively. $\Delta E=E_{\mathrm{S}}^{F,s}-E_{\mathrm{I}}^{F,s}$ and $\Delta\gamma'=\gamma_{\mathrm{S}}'-\gamma_{\mathrm{I}}'$. Formation energies are referenced from that for substitutional B at slab center by setting it zero.

B position	Surface	Third layer	Fifth layer	Center
$E_{\mathrm{I}}^{F,s}$	−1.65	−0.28	0.00	0.02
$E_{\mathrm{S}}^{F,s}$	−1.51	−0.02	0.00	0.00
ΔE	0.13	0.26	0.00	−0.02
γ_{I}'	2.44	3.12	3.26	3.31
γ_{S}'	2.59	3.34	3.35	3.35
$\Delta\gamma'$	0.15	0.22	0.09	0.04

rived in Sec. III, are provided in Table II. Differently from the bulk case, we have obtained the positive ΔE values for B impurity near the surface, that is, the preferential B position near the surface is interstitial rather than substitutional. In addition, we have found that the formation energies at the surface are lower by 1.52 eV and 1.67 eV than in bulk, for substitutional and interstitial B impurities, respectively. For both interstitial and substitutional cases, the formation energy decreases as the B position gets close to the surface. Accordingly, the substitutional B impurities in bulk have a tendency to segregate into the interstitial positions at the surface, which is in agreement with recent neutron autoradiography experiment.[28] These findings can also be interpreted in terms of interface energy instead of formation energy. The surface energies, γ_{I}' and γ_{S}', exhibit exactly the same behaviors as their corresponding formation energies, $E_{\mathrm{I}}^{F,s}$ and $E_{\mathrm{S}}^{F,s}$. For both interstitial and substitutional cases, the surface energies decrease as B impurities get close to the free surface. This analysis indicates that segregation of B impurities is the direct reflection that B impurities minimize the surface energy as they come out to the free surface. This result seems reasonable because the surface energy is already included in the total energy and thus in the calculation of formation energy. However, it is a noticeable result in the sense that the boundary energy determines the stability of total system.

Combining the bulk and the surface results for B impurities in α-Fe, it is deduced that both substitutional-to-substitutional and interstitial-to-interstitial diffusion mechanism coexist inside the bulk but the interstitial-to-interstitial diffusion becomes dominating near the free surface. In this process, it is thought to be possible that the dissociative diffusion,[18] namely, the dissociation of a substitutional B into an interstitial B plus a vacancy, occurs.

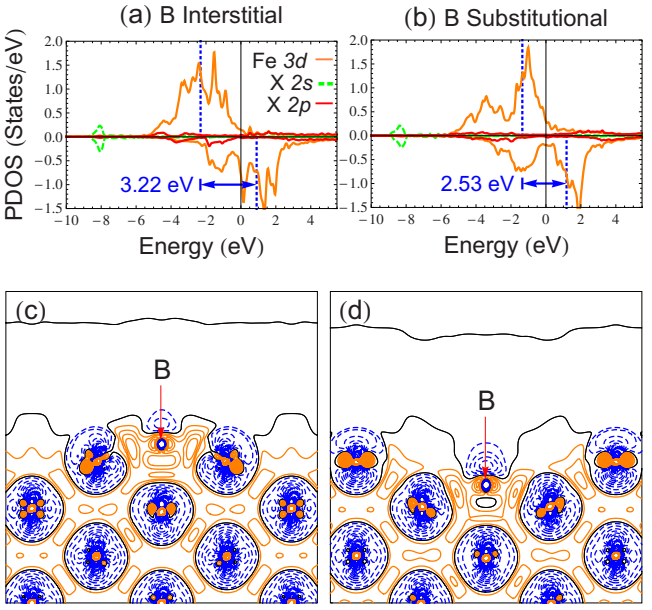

FIG. 6. (Color online). (a) PDOS for interstitial B at (100) surface in α-Fe. (b) PDOS for substitutional B at (100) surface α-Fe. (c) Bond charge density for interstitial B at (100) surface in α-Fe. (d) Bond charge density for substitutional B at (100) surface in α-Fe. Dotted (blue) lines in (a) and (b) indicate the center of Fe 3d up and down bands. Solid (orange) and dashed (blue) lines in (c) and (d) stand for positive and negative bond densities, respectively.

Plotted in Fig. 6 are the PDOSs and the bond charge densities for B impurity at (100) surface in α-Fe. As compared with the bulk PDOSs, the strong B-Fe hybridization is much weakened and the spin imbalance between Fe 3d majority and minority bands are much enhanced for interstitial B. In contrast, for substitutional B, the weak B-Fe hybridization is still retained, and the spin polarization is almost unchanged as can be seen from the fixed valley of Fe 3d minority band at Fermi level. It is clearly seen that the interstitial B in Fig. 6(c) is displaced from the surface toward the vacuum

TABLE III. Magnetic moment [μ_{B}] inside Fe MT sphere (M), number of Fe 3d electrons inside MT sphere for up and down spin (d_{up} and d_{dn}), Fe 3d band center (electron volt) for up and down spin ($\mathcal{E}_{\mathrm{up}}$ and $\mathcal{E}_{\mathrm{dn}}$), and the difference of Fe 3d band centers ($\Delta\mathcal{E}=\mathcal{E}_{\mathrm{dn}}-\mathcal{E}_{\mathrm{up}}$). $\mathrm{Fe}_{b,\mathrm{I}}$ and $\mathrm{Fe}_{b,\mathrm{S}}$ stand for the nearest Fe atoms for interstitial and substitutional B in Bulk α-Fe, respectively. $\mathrm{Fe}_{s,\mathrm{P}}$, $\mathrm{Fe}_{s,\mathrm{I}}$, and $\mathrm{Fe}_{s,\mathrm{S}}$ stand for Fe atom at (100) surface in pure α-Fe, and the nearest Fe atom for interstitial and substitutional B at (100) surface, respectively.

	M	d_{up}	d_{dn}	$\mathcal{E}_{\mathrm{up}}$	$\mathcal{E}_{\mathrm{dn}}$	$\Delta\mathcal{E}$
$\mathrm{Fe}_{b,\mathrm{I}}$	1.67	3.52	1.85	−1.55	0.51	2.07
$\mathrm{Fe}_{b,\mathrm{S}}$	2.09	3.70	1.61	−1.54	0.95	2.49
$\mathrm{Fe}_{s,\mathrm{P}}$	2.79	4.02	1.26	−2.47	0.82	3.29
$\mathrm{Fe}_{s,\mathrm{I}}$	2.54	3.90	1.37	−2.32	0.90	3.22
$\mathrm{Fe}_{s,\mathrm{S}}$	2.01	3.65	1.63	−1.35	1.18	2.53

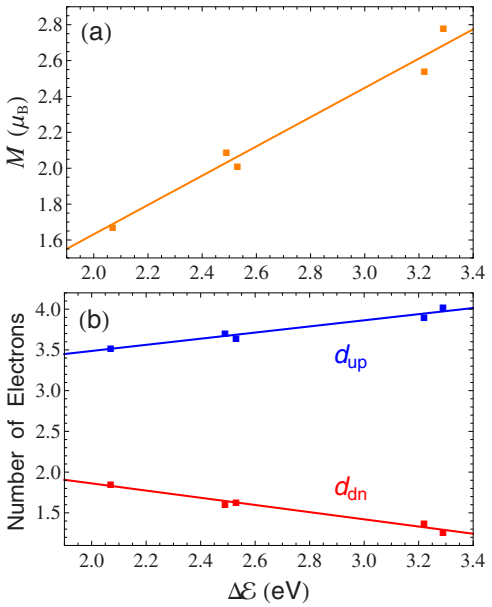

FIG. 7. (Color online). (a) Magnetic moment inside Fe MT sphere, M vs the difference of Fe 3d band centers, $\Delta\mathcal{E}=\mathcal{E}_{dn}-\mathcal{E}_{up}$, as presented in Table III. (b) Number of Fe 3d electrons inside MT sphere, d_{up} and d_{dn} vs $\Delta\mathcal{E}$, as presented in Table III.

whereas the substitutional B in Fig. 6(d) from the surface toward the subsurface layer. In consequence, the B-Fe distance for the interstitial B is enhanced from 3.39 to 3.90 a.u. whereas that for the substitutional B is reduced from 4.52 to 3.93 a.u. As the free surface is introduced, the geometrical pressure on interstitial B impurity is much relaxed and the B-Fe bonding strength is determined under this relaxed geometrical constraint. On the other hand, the geometrical asymmetry induced by the free surface provides substitutional B impurity with more degrees of freedom to move toward the subsurface layer. Figure 6(c) shows that the positive bond density of interstitial B is extended to the nearest Fe core. In contrast, for the substitutional B in Fig. 6(d), the positive bond density of its nearest Fe is more or less isolated inside the negative bond density and directed toward its neighboring Fe atoms along the contour valleys of negative bond density. This implies that the interstitial B-Fe bonding is still stronger than the substitutional B-Fe bonding as indicated by the B-Fe distances.

To understand the surface magnetism of Fe-B alloy system, we provide the magnetic moment of Fe atoms, the number of Fe 3d electrons, and the Fe 3d band centers in Table III. The band center represents the center of gravity and approximately indicates the energy level at which the delta peaklike atomic energy levels are broadened when atoms form solids and their orbitals are overlapped. Hence, the difference between up and down band centers effectively describes the exchange energy splitting $\Delta\mathcal{E}$, which corresponds to the magnetic moment, M, times the intra-atomic exchange-correlation interaction, I_{XC} of Fe 3d electrons. Indeed, as shown in Fig. 7, it is clearly seen that the magnetic moment inside Fe MT sphere is proportional to $\Delta\mathcal{E}$ and the corresponding I_{XC} is evaluated to be 1.23 eV. The magnetic moments of the nearest Fe atoms of interstitial and substitutional B at (100) surface are found to be $2.54\mu_B$ and $2.01\mu_B$, respectively. These correspond to 52.1 % enhanced and 3.8 % reduced values from the corresponding magnetic moments in bulk α-Fe. On the other hand, these surface magnetic moments correspond to 9.0% and 28.0% reduced values from the magnetic moment, $2.79\mu_B$, of Fe at (100) surface in pure α-Fe. For interstitial B, the magnetic-moment enhancement by the increased spin imbalance and the localization of Fe 3d state at the surface overcomes the magnetic-moment reduction by the B-Fe hybridization. In contrast, for substitutional B, those effects on Fe 3d state are much weakened by the screening of other Fe atoms at the surface, and the B-Fe hybridization contribution to the magnetic moment becomes more effective.

V. CONCLUSION

New formalism for the formation-energy calculation in a general interface is developed and applied to α-Fe with B impurities. We have found that B impurities in α-Fe prefer the substitutional position inside the bulk but the interstitial position near the surface. Both formation and surface energies of Fe-B system are found to decrease as B impurities get close to the free surface. It is thus expected from thermodynamic energetics that B impurities will segregate toward the free surface, thereby realizing the surface stability in boron steels. In bulk α-Fe, the solution type of B impurity is determined by the geometrical factors rather than the chemical bonding factors. In slab α-Fe, the geometrical pressure induces B impurities to segregate toward the surface. In this process, the boundary energy determines the stability of total system.

Embracing the bulk and the surface results, it is deduced that, deep inside the bulk α-Fe, both substitutional-to-substitutional and interstitial-to-interstitial diffusion coexist while, near the free surface, interstitial-to-interstitial diffusion becomes dominating. In the intermediate region, substitutional-to-substitutional diffusion can undergo a transition to interstitial-to-interstitial diffusion, and thereby it is thought that the dissociation of a substitutional B into an interstitial B plus a vacancy can effectively occur.

ACKNOWLEDGMENTS

This work was supported by the NRF (2009-0079947), the steel science project of POSCO, the NRF international cooperation program (KSRCP-2008-08), and by the WCU program (Project No. R32-2008-000-10147-0) of NRF.

*bimin@postech.ac.kr
†sekk@postech.ac.kr

[1] F. B. Pickering, *Physical Metallurgy and the Design of Steels* (Applied Science, London, 1978).
[2] *Boron in Steel*, edited by S. K. Banerji and J. E. Morral, Proceedings of the International Symposium on Boron Steels (AIME, Warrendale, PA, 1980).
[3] R. M. Goldhoff and J. W. Spretnak, J. Met **9**, 1278 (1957).
[4] L. Karlsson, H.-O. Andrén, and H. Nordén, Scr. Metall. **16**, 297 (1982).
[5] H. K. D. H. Bhadeshia and L.-E. Svensson, Proceedings of the International Conference on Modeling and Control of Joining Processes, edited by T. Zacharia (American Welding Society, Orlando, FL, 1993), pp. 153–160.
[6] F. P. A. Robinson and W. G. Scurr, Corrosion **33**, 408 (1977).
[7] R. I. Presser and R. McPherson, Scr. Metall. **11**, 745 (1977).
[8] R. Wu, A. J. Freeman, and G. B. Olson, Science **265**, 376 (1994).
[9] P. E. Busby, M. E. Warga, and C. Wells, J. Met. **5**, 1462 (1953).
[10] P. E. Busby and C. Wells, J. Met. **6**, 972 (1954).
[11] A. K. Shevelev, Dokl. Akad. Nauk SSSR **123**, 453 (1958).
[12] P. M. Strocchi, B. A. Melandri, and A. Tamba, Nuovo Cimento B **51**, 1 (1967).
[13] R. R. Hasiguti and G. Kamoshita, J. Phys. Soc. Jpn. **9**, 646 (1954).
[14] W. R. Thomas and G. M. Leak, Nature (London) **176**, 29 (1955).
[15] F. N. Tavadze, I. A. Bairamashvili, and V. S. Metreveli, Soobsch. Akad. Nauk. Gruzin. SSR **40**, 401 (1965).
[16] W. Wang, S. Zhang, and X. He, Acta Metall. Mater. **43**, 1693 (1995).
[17] D. H. R. Fors and G. Wahnström, Phys. Rev. B **77**, 132102 (2008).
[18] Y. Hayashi and T. Sugeno, Acta Metall. **18**, 693 (1970).
[19] A. Lucci and G. Venturello, Scr. Metall. **5**, 17 (1971).
[20] M. Weinert, E. Wimmer, and A. J. Freeman, Phys. Rev. B **26**, 4571 (1982).
[21] P. Blaha, K. Schwarz, G. K. H. Madsen, D. Kvasnicka, and J. Luitz, *WIEN2k* (Technische Universität Wien, Austria, 2001).
[22] J. P. Perdew, K. Burke, and M. Ernzerhof, Phys. Rev. Lett. **77**, 3865 (1996).
[23] D. E. Jiang and E. A. Carter, Phys. Rev. B **67**, 214103 (2003).
[24] N. L. Peterson, J. Nucl. Mater. **69-70**, 3 (1978).
[25] The energy difference between octahedral and tetrahedral sites amounts to 0.70 eV.
[26] C. Domain, C. S. Becquart, and J. Foct, Phys. Rev. B **69**, 144112 (2004).
[27] $y=a/x+b$ where a and b are the constants to be determined, and x is the number of Fe atoms in the unit cell. $x=10\,000$ corresponds to 20 wt. ppm of boron solution in α-Fe.
[28] D. J. Mun, M.S. thesis, POSTECH, 2008.